HHS Public Access

Author manuscript

Acta Biomater. Author manuscript; available in PMC 2020 January 01.

Published in final edited form as:

Acta Biomater. 2019 January 01; 83: 109–118. doi:10.1016/j.actbio.2018.10.037.

Biomimetic Recyclable Microgels for On-Demand Generation of Hydrogen Peroxide and Antipathogenic Application

Hao Meng[1], **Pegah Kord Forooshani**[1], **Pratik U. Joshi**[2], **Julie Osborne**[1], **Xue Mi**[2], **Christa Meingast**[3], **Rattapol Pinnaratip**[1], **Jonathan Kelley**[1], **Ameya Narkar**[1], **Weilue He**[1], **Megan C. Frost**[1], **Caryn L. Heldt**[2], and **Bruce P. Lee**[1]

[1]Department of Biomedical Engineering, Michigan Technological University, Houghton, MI 49931, USA

[2]Department of Chemical Engineering, Michigan Technological University, Houghton, MI 49931, USA

[3]Department of Civil and Environmental Engineering, Michigan Technological University, Houghton, MI 49931, USA

Abstract

Microgels that can generate antipathogenic levels of hydrogen peroxide (H_2O_2) through simple rehydration in solutions with physiological pH are described herein. H_2O_2 is a widely used disinfectant but the oxidant is hazardous to store and transport. Catechol, an adhesive moiety found in mussel adhesive proteins, was incorporated into microgels, which generated 1–5 mM of H_2O_2 for up to four days as catechol autoxidized. The sustained release of low concentrations of H_2O_2 was antimicrobial against both gram-positive (*Staphylococcus epidermidis*) and gram-negative (*Escherichia coli*) bacteria and antiviral against both non-enveloped porcine parvovirus (PPV) and enveloped bovine viral diarrhea virus (BVDV). The amount of released H_2O_2 is several orders of magnitude lower than H_2O_2 concentration previously reported for antipathogenic activity. Most notably, these microgels reduced the invectively of the more biocide resistant non-envelope virus by 3 log reduction value (99.9% reduction in infectivity). By controlling the oxidation state of catechol, microgels can be repeatedly activated and deactivated for H_2O_2 generation. These microgels do not contain a reservoir for storing the reactive H_2O_2 and can potentially function as a lightweight and portable dried powder source for the disinfectant for a wide range of applications.

Graphical Abstract

bplee@mtu.edu.

Competing financial interests

The authors declare no competing financial interests.

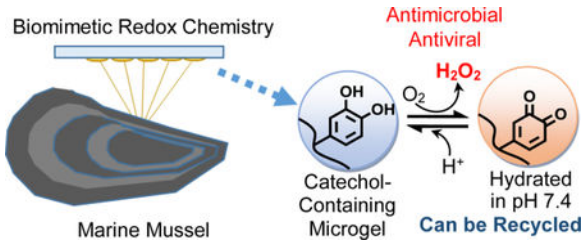

Keywords

dopamine; recyclable microgels; hydrogen peroxide; antimicrobial; antiviral

1. Introduction

Hydrogen peroxide (H_2O_2) is a strong oxidizing agent [1]. Depending on the concentration, the exposure time, and the form of delivery (i.e., liquid or gas), H_2O_2 has been demonstrated to function as an effective, broad-spectrum biocide in many industrial and biomedical applications [2, 3]. H_2O_2 is an attractive disinfectant because it decomposes into biocompatible degradation products (oxygen and water) [2]. Solutions with a H_2O_2 concentration greater than 3% w/w (0.9 M) have been reported to kill both gram-positive (*Staphylococcus*, *Streptococcus*, *Enterococcus*) and gram-negative (*Pseudomonas*, *Klebsiella*, *Escherichia*) bacteria [2, 4]. Certain types of gram-positive bacteria (e.g., *Staphylococcus*) secreted catalase to decompose H_2O_2 into water and oxygen, which effectively decrease H_2O_2 concentration [5]. Therefore, higher concentration (>3%) of H_2O_2 was necessary to inhibit or kill these bacteria [6]. In contrast, the growth of bacteria that do not secrete catalase (e.g., oral *Streptococcus*) can be inhibited at a concentration as low as 0.1 mM [7]. H_2O_2 solutions with similar concentrations (1–3 % w/w) also effectively inactivated enveloped viruses (e.g., influenza and rabies virus) for the development of vaccines [1, 8]. Non-enveloped viruses (e.g., poliovirus) are typically more resistant to biocides compared to enveloped viruses and aqueous H_2O_2 solutions are not sufficient to inactivate most non-enveloped viruses [9]. Vaporized H_2O_2 is an ideal alternative sterilization method to deliver gaseous H_2O_2 to inactivate non-enveloped viruses [10–12]. However, this sterilization method requires specialized equipment (i.e., a generator and a vaporizer) for vapor formation, which is not cost effective [2, 13].

H_2O_2 is typically stored as an aqueous solution and is commercially available in concentrations ranging from 3–90% (w/w) [9]. However, it is highly challenging to transport and store H_2O_2 solutions. Diluted solutions are bulky and not easily portable, while solutions with a concentration greater than 59% are hazardous to transport due to the unstable and explosive nature of concentrated peroxide [2]. Researchers are exploring alternative methods to increase the stability of H_2O_2 in an aqueous solution for the convenience of storing it at ambient temperature. These methods include the addition of peroxide stabilizing additives [14], complex formation (e.g., urea-H_2O_2 complex) [15], and encapsulation of H_2O_2 into polymer matrices (e.g., sol-gel silica hydrogels) [3]. However, these stabilization methods only decreased the decomposition rate of H_2O_2 without inhibiting reactivity, resulting in mixed results.

Unlike the existing approaches that focus on stabilizing H_2O_2 for prolonged storage, we are exploiting a unique, biomimetic reduction-oxidation (redox) chemistry to design microgels that can be repeatedly activated to generate H_2O_2 on demand. Marine mussels secrete adhesive proteins that enable these organisms to bind to various surfaces underwater [16]. One unique structural component of these proteins is a catechol-containing amino acid, 3,4-dihydroxyphenylalanine (DOPA), which is capable of binding to surfaces via various strong interfacial interactions [17]. DOPA can transition between its reduced (i.e. catechol) and oxidized (i.e., quinone) forms depending on the solution pH and the presence of an oxidant (e.g., molecular oxygen, periodate, tyrosinase, etc.) [18–20]. As catechol oxidizes, H_2O_2 is generated as a byproduct during the process [21]. Here, we exploit this unique redox 3 active adhesive moiety to design microgels that generate H_2O_2 on demand for antimicrobial and antiviral applications (Figure 1).

2. Experimental methods

2.1. Materials

N-Hydroxyethyl acrylamide (HEAA), TWEEN®80, SpanTM80, acetone, phosphate buffered saline (PBS, BioPerformance certified, pH 7.4), horse serum, and bovine liver catalase were purchased from Sigma Aldrich (St Louis, MO). Sodium phosphate monobasic monohydrate, sodium phosphate dibasic anhydrous, and methylene bis-acrylamide (MBAA) were purchased from Acros Organics (Fair Lawn, New Jersey). VA-086 was purchased from Wako Chemicals (Richmond, VA). Dimethyl sulfoxide (DMSO), hexanes and sodium dodecyl sulfate (SDS) were purchased from VWR (Radnor, PA). 12 M hydrochloric (HCl) acid was purchased from Fisher Scientific (Pittsburg, PA). DMEM (with 4.5 g/L glucose and glutamine, without sodium pyruvate) was obtained from Corning Cellgro (Tewksbury, MA). H_2O_2 (30% stock solution) was from Avantor (Center Valley, PA). Pierce Quantitative Peroxide Assay Kit with sorbitol and dihydroethidium (DHE) was purchased from Thermo Scientific (Rockford, IL). Dopamine methacrylamide (DMA) was synthesized following published protocols[22]. Mueller Hinton Agars (28 ml fill, 15×100 mm), tryptic soy broth, and astral inoc loop (10 μL, blue, sterilized) were purchased from Hardy Diagnostics (Santa Maria, CA). Anprolene® gas sterilization and gas refills (ethylene oxide) were purchased from Andersen Sterilizers, Inc. (Haw River, NC). Medium essential media (MEM) 1×, sodium bicarbonate (7.5%), penicillin/streptomycin and 0.25% trypsin/EDTA for cell propagation were purchased from Life Technologies (Carlsbad, CA). Sodium pyruvate solution (100 mM) was purchased from Lonza (Walkersville, MD). Fetal bovine serum (FBS, Canada origin) was purchased from HyCloneTM GE Healthcare (Pittsburg, PA). 3-(4,5-dimethyl-2-thiazolyl)-2,5-diphenyl-2H-tetrazolium bromide (MTT) was purchased from Alfa Aesar (Haverhill, MA). Porcine kidney cells (PK-13, CRL-6489), bovine testis cells (BT-1, CRL-1390), *Staphylococcus epidermidis* (*S. epi*, ATCC 12228) and *Escherichia coli* (*E. coli*, ATCC 11775) were purchased from American Type Culture Collection (ATCC, Manassas, Virginia). Enveloped bovine viral diarrhea virus (BVDV) was purchased from USDA APHIS and porcine parvovirus (PPV) was a generous gift from Dr. Ruben Carbonell, North Carolina State University. Phosphate buffer (PB) solutions with different pH (6.7–8.2) was prepared by mixing different volume percentages of 0.2 M stock solution of sodium phosphate monobasic and sodium phosphate dibasic, then further diluted to a 0.1 M

concentration using DI water[23]. pH 3.5 PBS was prepared following procedure found in European Pharmacopoeia (Chapter 4. Reagents) [24].

2.2. Preparation of microgels

Microgels were prepared by mixing 70 mL hexane, 500 μL SpanTM80 and 100 μL TWEEN®80 in a rubber plug-sealed flask and stirred vigorously under a nitrogen-rich atmosphere for 30 min. Polymer precursor solutions were prepared by mixing 1 M of HEAA with 0–10 mol% of DMA, 6 mol% of MBAA and 4 mol% of VA086 relative to HEAA in DI water. The precursor solutions were frozen for 30 min and degassed 3 times by backfilling with N2. Then the precursor solutions were added to the surfactant mixture drop by drop using a syringe. The reaction was initiated by irradiating UV light (365 nm, UVP UVGL-25, Analytik Jena) on the side of the flask and rigorous stirring for 4 h (Scheme S1). The microgels were collected by filtration and washed with acetone and isopropyl alcohol in succession until the microgels became white. The microgels were dried under vacuum for overnight and further washed with DI water (pH 3.5) for 30 min. Microgels were collected through centrifugation at 5,000 rpm for 10 min and lyophilized to yield dried microgel powder.

2.3. Characterization of microgels

Microgels were dried under vacuum and characterize using FTIR spectroscopy (Perkin Elmer Spectrum One spectrometer). The particle size of microgels were determine in both dried and swollen states. Dried microgels were coated with 2 nm thick Pt/Pd coating and characterized with FE-SEM (Hitachi S-4700). Dried microgels (10 mg/mL) were equilibrated in either pH 3.5 DI water or PBS (pH 7.4) for 1 h. 10 μL of microgels suspension was added onto a glass slide and covered with a coverslip. The morphology of the swollen microgels was imaged under light microscope (Olympus BX51). The sizes of the microgels were measured using ImgeJ software. The average size and size distribution of the microgels were calculated based on at least 200 microgels for each microgel composition.

2.4. H_2O_2 concentration determination

Microgels were suspended in 725 μL of the desired hydrating fluid (pH 7.4 or 3.5 PBS, pH 6.7–8.2 PB) and incubated for up to 96 h with gentle agitation on a shaking plate. H_2O_2 concentration was quantified by using the Quantitative Peroxide Assay Kit following published protocols[25]. A standard curved was constructed using solution containing 0–1 mM of H_2O_2 (double diluted to 10 concentrations). To determine the effect of catalase on the H_2O_2 generation, 25 mg of 10 mol% DMA microgel was suspended in 225 μL of PBS (pH 7.4) and mixed with 500 μL of PBS containing 1 mg/mL of bovina liver catalase (2000–5000 U/mg), and incubated at 37°C.

2.5. Recyclability of microgel

25 mg of microgels were equilibrated with 725 μL of DI water (pH 3.5) for 12 h at room temperature. The microgels were then centrifuged at 5,000 rpm for 5 min and the supernatant was assayed to determine H_2O_2 concentration. The microgels were washed 3

times in PBS (pH 7.4) and further incubated in PBS for 12 h and centrifuged at 5,000 rpm for 5 min. The supernatant was assayed to determine H_2O_2 concentration. This process was repeated 5 times to determine the amount of H_2O_2 generated after successive incubation in DI water (pH 3.5) and PBS (pH 7.4). Recyclability between PBS buffered at pH 3.5 and pH 7.4 was also performed in a similar manner.

2.6. Staining microgel with DHE

The ability for the microgel to generate superoxide anion ($O_2^{\bullet -}$) was determined by DHE staining [26]. 25 mg of microgel was incubated in 725 μL of PBS (pH 7.4) at 37°C for 24h. The samples were further incubated with DHE (10μM in PBS) for 30 min at 37°C, while being protected from ambient light. Samples were imaged using a fluorescence microscope (excitation 480–520 nm).

2.7. UV-vis characterization of catechol oxidation

Linear polymer containing 10 mol% of DMA was prepared using the microgel fabrication protocol without the MBAA cross-linker. The polymer was dialyzed with pH 3.5 DI water for 3 days and freeze dried. The polymer was solublized in either DI water (pH 3.5) or PBS (pH 7.4) with a DMA concentration of 0.36 mM and incubated at 37°C for 72 h. At a predetermined time, the UV-vis spectra (250 to 700 nm; PerkinElmer Lambda35) of the solution was recorded at a scan rate of 960 nm/min using either DI water (pH 3.5) or PBS (pH 7.4) as the reference.

2.8. Antimicrobial activity of the microgels

Microgels were separated into 24-well tissue culture plates and sterilized using ethylene oxide. The antibacterial activity of the microgels was evaluated following published paper with minor modifications[27]. Both *S. epi* and *E. coli* grown on the stock plate were diluted by broth to a concentration of 100,000 CFU/mL. 25 mg of the sterilized microgels containing either 10 or 0 mol% of DMA were equilibrated with 225 μL of PBS (pH 7.4) for 5 min. 500 μL of bacteria suspended in broth solution was added to the microgel and the mixture was incubated at 37 °C. At a given time point, either a 10 μL (for *S. epi*) or 1 μL (for *E. coli*) loop was immersed into the mixture without touching the precipitated microgels and streaked onto agar plates, which were further incubated at 37°C for 24 h. H_2O_2 stock solution (30%, 9M) was diluted to the concentration of 10 mM and 1 mM using broth, which were directly incubated with both bacteria strains as positive control. The agar plates with colonies were photographed and the bacteria colonies were counted using ImageJ. The relative colony numbers were calculated following the equation below[28]:

$$\text{Relative colonies numbers } \% = N_m/N_c \times 100\%, \quad (1)$$

where N_m is the colony numbers formed from the bacteria exposed to the microgels and N_c is the colony numbers formed from the bacteria cultured in broth that did not contain any microgel. To determine the effect of catalase on the antimicrobial property of the microgel, catalase was added to PBS and the broth solution at a concentration of 1 mg/mL and

sterilized using cellulose acetate syringe filter (0.2 μm). The antimicrobial experiment was carried out as described above.

2.9. Antiviral property of microgels

25 mg of microgels were sterilized using ethylene oxide and equilibrated with 225 μL PBS (pH 7.4) for 5 min. 500 μL of log 6 MTT50/mL PPV or BVDV in PBS (pH 7.4) were added to the wells containing the equilibrated microgels and incubated at 37°C with 5% CO_2 and 100% humidity. At the designated time points, the microgels were separated from the virus suspension by centrifugation (6000 rpm for 5 min) in a Sorvall ST16R Centrifuge (Thermo Scientific, Pittsburg, PA) and the supernatants containing the treated PPV and BVDV were used to PK-13 and BT-1 cells, respectively. The titer of virus was determined by colorimetric MTT mediated cell viability assay, as described previously [29, 30]. Briefly, either 8×10^4 cells/ml (for PK-13 cells) or 2.5×10^5 cells/ml (for BT cells) were seeded in 96-well plate for 24 h. 25 μL of virus supernatant was added to the wells in quadruplicate, with a serial dilution of 1:5 across the plate for 5 days. MTT (5 mg/mL in PBS, pH 7.2) was added to the wells for 4 h. Then, 10% SDS (pH 2) was added to the wells to lyse the cells for 24 h. The absorbance was determined using a Synergy Mx microplate reader (BioTek, Winoski, VT) at 550 nm.

The 50% infectious dose of virus was found by determining 50% uninfectious cell absorbance and labeled as the MTT_{50} [29]. Log reduction values (LRV) were calculated by[30]:

$$LRV = -\log\left(\frac{C_i}{C_f}\right) \quad (2)$$

where C_i and C_f are intial and final concentrations, respectively. For comparison purposes, the two viruses were incubated with 3–292 mM of H_2O_2 at 37°C for 12 h and the viral titer values were determined based on the viability of the respective indicator cell lines using MTT assay as described above.

2.10. Microgel mesh size calculation

The mesh size (ξ) was calculated using the following equation [31]:

$$\xi = v_s^{-1/3}\left(\frac{2C_n\overline{M}_c}{M_n}\right)^{1/2} l \quad (3)$$

where v_s is the polymer volume fraction in the swollen microgel, C_n is the Flory characteristic ratio, $\overline{M}_c$ is the average molecular weight between crosslink, and M_n is molecular weight for the repeating unit (115 Da for HEAA), and l is the length of the bond along the polymer backbone (1.54 Å for vinyl polymers)[31]. v_s was calculated using the following equation [32]:

$$v_s = \frac{V_p}{V_s} \quad (4)$$

where V_p and V_s are the volume of the hydrogels in the dried and swollen states, respectively. The average particle size for microgels in the dried and swollen (PBS pH 7.4) states (Table S1) were used as the diameter of a sphere to estimate V_p and V_s, respectively. C_n of polyvinyl alcohol (8.3) [33] was used as it has the same hydroxyl functional group as polyHEAA. $\overline{M}_c$ was calculated using the Flory-Rehner equation [34]:

$$\overline{M}_c = \frac{\rho_p V_{H20}\left(v_s^{1/3} - v_s/2\right)}{\ln(1 - v_s) + v_s + \chi v_s^2} \quad (5)$$

where ρ_p is the density of polyHEAA (1.31 g/cm^3) [35], V_{H_2O} is the molar volume of water (18.1 mol/cm^3) and χ is the Flory-Huggins parameter for pHEAA and water, which approaches 0.5 when fully hydrated [36].

2.11. Statistical analysis

One-way analysis of variance (ANOVA) with Tukey HSD analysis and student t-test were performed for comparing means of multiple groups and two groups, respectively, using a p-value of 0.05.

3. Results and discussion

3.1. Microgel preparation and characterization

Catechol-containing microgels were prepared by photo-initiated polymerization of up to 10 mol% of DMA, a hydrophilic monomer (HEAA) and a bifunctional crosslinker (MBAA) in an emulsion. DMA contains a catechol moiety that mimics the redox active DOPA side chain (Figure S1). These microgels exhibited characteristic peaks in Fourier transform infrared (FTIR) spectra associated with catechol (Figure S2) [37]. From field emission scanning electron microscope (FE-SEM) images (Figure 1b, Figure S3), dried microgels appeared rounded in shape with an average diameter of around 10 μm regardless of composition (Table S1). After hydrating in a liquid solution, the microgels increased in size and retained the spherical shape (Figure S4, Figure 1c, and Table S1). Microgels containing 0 mol% DMA enlarged by nearly 3 fold after equilibrating in solutions. On the other hand, the sizes of the swollen microgels decreased with increasing DMA content. Microgels containing 5 and 10 mol% DMA only increased 1.5 fold. The limited size change in DMA containing microgels was due to the extensive intermolecular interaction (i.e., **π-π** interaction, hydrogen bonding, etc.) between network-bound catechol moieties [38], which significantly restricted the swelling of these microgels.

3.2. Autoxidation of DMA containing microgels

Catechol moieties readily autoxidize in an oxygenated solution at neutral or alkaline pH [38, 39]. Microgels containing 10 mol% of DMA remained white in color when they were incubated in deionized (DI) water acidified to pH 3.5 (Figure 1d), indicating the catechol group remained in its reduced state at acidic pH. Microgels only became red in color when they were equilibrated in phosphate buffer saline (PBS) at pH 7.4 (Figure 1e), corresponding to catechol oxidation. UV-vis spectrum of polymer containing 10 mol% DMA dissolved in DI water (pH 3.5) exhibited only a single peak at 280 nm (Figure S5), corresponding to the characteristic peak of the reduced form of catechol [40]. The spectrum remained unchanged even after 72 h of incubation, confirming that catechol did not oxidize at pH 3.5. In contrast, the absorbance intensity of the polymer spectrum started to increase within 1.5 h of incubation in PBS. The characteristic peak for dopamine quinone (λ_{max} = 392) [41] was not directly observed, potentially due to the rapid formation and decay of this transient intermediate in basic pH [42]. The drastic increase in the absorbance between 300 nm and 350 nm corresponded favorably to the formation of α,β-dehydrodopamine (λ_{max} = 322 nm) [43], a more stable oxidation product formed through the charge transfer complex between catechol and quinone [19].

3.3. H_2O_2 generation under different conditions

We investigated the effect of DMA concentration, microgel concentration, incubation temperature, and pH of the hydrating fluid on the release of H_2O_2 (Figure 2). Dried microgels with various amounts of DMA content (0–10 mol%) were incubated in PBS (pH 7.4) at 37°C. For microgel containing 10 mol% DMA, more than 740 μM of H_2O_2 was detected within 1.5 h of incubation. Molecular oxygen oxidizes catechol to semiquinone and quinone, while generating superoxide anion ($O_2^{\bullet-}$) during the process [44]. $O_2^{\bullet-}$was detected in DMA-containing microgels using the superoxide indicator, DHE, which was oxidized to red-fluorescence specifically by $O_2^{\bullet-}$(Figure S6). However, no red fluorescent signal was captured in 0 mol% DMA microgels, indicating that $O_2^{\bullet-}$was generated through catechol autoxidation. $O_2^{\bullet-}$can further oxidize catechol to generate H_2O_2 or react with proton ions to generate H_2O_2 [45]. H_2O_2 concentration reached a maximum of nearly 4 mM after 24h and the microgels continued to generate over 4 mM of H_2O_2 for up to 96 h (Figure 2a). Given the short half-life of H_2O_2 at physiological pH and temperature [46], H_2O_2 was continuously being generated by these microgels. Increasing DMA content increased the amount of released H_2O_2 from the microgels. No H_2O_2 was detected for microgels that did not contain DMA (e.g., 0 mol% DMA), indicating that the network-bound catechol was the source for the detected H_2O_2. Similarly, H_2O_2 concentration increased proportionally with increasing microgel concentration (Figure 2b).

These observations differed from the release profile of H_2O_2 from our previously reported macro-size hydrogel discs (1 cm diameter, 2–4 mm thick), where H_2O_2 concentration did not increase proportionally with increasing DMA content or hydrogel concentration [38]. H_2O_2 generated by the macro-size hydrogel was largely diffusion limited and trapped within its bulk, and increased crosslinking density and thickness limited liquid exchange between the hydrogel network and the extract. However, diffusion of H_2O_2 from microgels was not an issue due to a significantly higher surface-to-volume ratio (~100 times higher), which

facilitated the release of H_2O_2. Microgels generated nearly an order of magnitude higher H_2O_2 when compared to the macro-size hydrogels (Figure S7).

H_2O_2 concentration generated from DMA-containing microgels increased with increasing incubation temperature (Figure 2c). Although the decomposition rate of H_2O_2 increases with increasing temperature [47], the oxidation rate of catechol as well as the molecular diffusion was accelerated at the same time [48]. After 1.5 h of incubation, H_2O_2 concentrations increased with incubation temperature, and the highest concentration was measured at 60°C (2 mM). This indicated that the rate of catechol oxidation and release increased with temperature. With prolonged incubation time, H_2O_2 concentrations plateaued, implying that an equilibrium between H_2O_2 production and decomposition was achieved. In general, the H_2O_2 equilibrium concentration increased with incubation temperature. However, the equilibrium concentration measured at 60°C (3.5 mM) was lower when compared to that of 37°C (4 mM), indicating that the rate of H_2O_2 decomposition was higher at the elevated temperature. H_2O_2 production from microgels at 4°C increased slowly over time and reached around 1 mM after 96 h of incubation, without a clear equilibrium being achieved.

Phosphate buffer (PB) solutions (without sodium chloride (NaCl)) with different pH (6.7–8.2) were prepared to assess the effect of pH on H_2O_2 generation (Figure 2d). DMA-containing microgels initially generated a higher amount of H_2O_2, when they were incubated at an elevated pH level. After 1.5 h, microgels generated the highest amount of H_2O_2 (~1.8 mM) at pH 8.2, which is 1.3 and 3.4 fold higher when compared to those generated at pH 7.4 and 6.7, respectively. However, unlike microgels that were incubated in PBS (pH = 7.4) that generated H_2O_2 continuously for 96 h, H_2O_2 released from microgels incubated in PB (pH 7.4 and 8.2) reached a maximum after 24 hours and decreased over time. When hydrated in pH 6.7 PB, H_2O_2 was continuously generated and reached a peak concentration of 5.4 mM after 96 h. For comparison purposes, microgels were also incubated in pH 3.5 DI water. H_2O_2 was not detected during the entire 96 h incubation.

The pH and composition of the hydrating fluid greatly influenced the generation and decay of H_2O_2. In basic pH, catechol oxidized more rapidly and initially released a higher concentration of H_2O_2. However, the concentration of H_2O_2 decreased drastically over time because H_2O_2 is less stable at an elevated pH [49]. Additionally, covalent crosslinking via dimer formation and polymerization of catechol moieties occurs more rapidly at an elevated pH [42], which decreased the number of catechol that could be further oxidized to generate H_2O_2. We previously reported that chemical oxidant-induced oxidation and crosslinking of catechol exhibited a similar initial burst release of H_2O_2 followed by a drastic reduction in measured H_2O_2 over time [50]. Microgels did not release H_2O_2 at pH 3.5 as catechol remained in its reduced form as demonstrated from the UV-vis spectra (Figure S5a). A pH of 6.7 appeared to be more suitable for sustained release of H_2O_2, which combined a moderate rate of catechol oxidation and a relatively slower H_2O_2 decomposition rate [51]. Interestingly, H_2O_2 concentration profiles differed significantly for microgels hydrated in PB and PBS, even though both solutions were buffered at pH 7.4 (Figure S8). PBS contained 138 mM of NaCl, which may have reduced the rate of catechol oxidation [52] and prevented subsequent oxidative crosslinking. Microgels incubated in PBS generated significantly lower

amount of H_2O_2 (~50% after 1.5 h) when compared to those incubated in PB. Additionally, the presence of the chloride ion may have decreased the rate of H_2O_2 decomposition [53].

3.4. Recyclability of the microgel

To determine if the microgels could be repeatedly activated and deactivated, microgels containing 10 mol% of DMA were sequentially incubated in PBS (pH 7.4) and pH 3.5 DI water for 12 h during each incubation cycle (Figure 3). The microgels are not water soluble and can be easily separated from the hydrating solution by centrifugation or filtration for repeated use. Cycling between the two pH levels repeatedly activated and deactivated the microgels for H_2O_2 generation. In each cycle of incubation at pH 7.4, microgels generated around 1.2 mM of H_2O_2 and the concentration did not change significantly over 5 cycles ($p > 0.05$). On the other hand, no H_2O_2 was detected when the microgels were incubated at pH 3.5. Similar H_2O_2 generation was observed when the microgels were repeatedly incubated in PBS buffered at pH 3.5 and 7.4 (Figure S9). When the microgels were initially oxidized in pH 7.4, microgels transformed from white to red in appearance (Figure 3b and c), indicating the oxidation of network-bound catechol to quinone. The oxidized DMA-containing microgels did not regain the initial white color after incubation in pH 3.5, instead became yellow in color (Figure 3d). These observations suggest that dopamine (white) in DMA was first transformed into dopamine quinone (red) when it was initially oxidized (Scheme 1). Our UV-vis data (Figure S5b) indicated the formation of α,β-dehydrodopamine (yellow) during autoxidation, potentially due to its increased stability at a basic pH when compared to dopamine quinone [54]. α,β-dehydrodopamine regained a catechol moiety that could be further oxidized to α,β-dehydrodopamine quinone, generating H_2O_2 during the process [50, 54]. The subsequent cycles of pH changes likely involved the oxidation and reduction of α,β-dehydrodopamine.

For DMA-containing microgels, the color change occurred rapidly (supplementary video), indicating rapid diffusion and exchange between the microgels and the surrounding solution. The ability to transition quickly between the two oxidation states is important for designing a rapidly responsive and reversible smart biomaterial. On the other hand, macro-size hydrogel required several days to exhibit similar color changes in response to changing solution pH (data not shown). The ability to be rapidly and repeatedly activated to release millimolar levels of H_2O_2 makes the microgels a suitable and recyclable source for the antipathogenic H_2O_2.

3.5. Antimicrobial property of the microgel

Both gram-positive (*S. epi*) and gram-negative (*E. coli*) bacteria were used to evaluate the antimicrobial property of the H_2O_2 releasing microgels. Both *S. epi* and *E. coli* (100,000 CFU/mL) were exposed to microgels containing either 0 or 10 mol% DMA at 37°C for up to 24 h, and the treated bacteria were streaked onto agar plates to determine their viability. For both bacteria strains, incubation with microgels containing 10 mol% DMA decreased the number of colonies formed over time, and no colony formation was observed after 24 h of incubation (Figure S10 and S11). When compared to the bacteria growth in the broth control, the relative colony numbers decreased to 19.9 ± 10.7% for *S. epi* exposed to microgels containing 10 mol% DMA within 6 h and reached 0% after 24 h (Figure 4a).

Similarly, the relative bacteria colony numbers for *E. coli* decreased to 5.3 ± 1.7% only after 3 h of incubation, and there was nearly no colony formation after 6 h (Figure 4b). These results indicated that H_2O_2 generated by DMA-containing microgel completely killed both bacteria strains within 24 h. The bacteria cultured with 0 mol% DMA microgels and in the broth without microgels demonstrated an increase in the number of colony forming unit overtime. In the absence of DMA-containing microgels, bacteria rapidly replicated and the relative bacteria colony numbers were around 100% within 6 h of incubation. When compared to the antimicrobial response to a single dose of H_2O_2, the efficacy of the DMA-containing microgels was equivalent to exposure to 1 mM of H_2O_2 (Figures S12 and S13, Table S2).

To confirm that the released H_2O_2 was responsible for the observed antimicrobial property, control experiments were carried out in the presence of bovine liver catalase. Catalase is an enzyme found in many living organisms that are exposed to air and catalyzes the decomposition of H_2O_2 into water and oxygen [55]. No H_2O_2 was detected for microgels containing 10 mol% of DMA when they were incubated with 0.7 mg/mL of catalase (2000–5000 U/mg; Figure S14). In the presence of catalase, DMA-containing microgels lost their antimicrobial properties as both bacteria strains readily replicated over 24 h of incubation (Figure S15). Adding catalase alone to the broth containing no microgel had no impact on the colony formation of the bacteria.

3.6. Antiviral property of the microgel

The ability for the DMA-containing microgel to inactivate virus was tested against both non-enveloped PPV and the enveloped BVDV. PPV and BVDV are standard viruses used by the Food and Drug Administration (FDA) to test virus removal operations in biotherapeutic production. These viruses were incubated with microgels containing either 0 or 10 mol% DMA at 37°C with a starting viral titer of 6 log10 MTT/ml. The viral titer values were determined based on the viability of indicator cell lines (PK-13 and BT-1 for PPV and BVDV, respectively) and measured with the cell proliferation dye MTT (Figure S16) [29]. DMA-containing microgels reduced the PPV titer value by nearly 3 log reduction value (LRV), which corresponds to a 99.9% reduced infectivity after 12 h of incubation (Figure 5). This value is approaching the Environmental Protection Agency and FDA limit of 4 log reduction for a virus inactivation method [56, 57]. Most impressively, DMA-containing microgels reduced the BVDV titer value by 4–5 LRV (99.99%−99.999% reduced infectivity) over the same time period. This result corroborates previous findings that enveloped viruses are more susceptible to inactivation by liquid H_2O_2 [1, 8]. For comparison purposes, the two viruses were exposed to a single dose of H_2O_2 at a concentration of 3–292 mM (Figure S17). 3 mM H_2O_2 was ineffective in inactivating these viruses and concentrations that were 1–2 orders of magnitude higher were required to inactivate these viruses. However, only a titer value of 1–1.8 LRV was achieved after 12 h of exposure.

Microgels containing 0 mol% DMA also demonstrated a 2 log reduction in the viral activity after 48 h (Figure 5). The particle size of PPV (18–26 nm)[58] and BVDV (40–60 nm)[59] are smaller than the estimated mesh size for microgels containing 0 mol% of DMA (70 nm, Table S3). It is possible that these viruses were able to diffuse into the microgel network

over time and were removed along with the microgel during centrifugation. Additionally, the envelope glycoproteins found on the surface of BVDV can potentially interact with the hydroxyl and amide functional groups found on polyHEAA backbone of the microgel through hydrogen bonding and be removed with the microgel [60].

Previous publications demonstrated that a single dose of H_2O_2 solution with a concentration greater than 1000 mM was necessary to kill both gram-positive and gram-negative bacteria [2, 4] and to inactivate enveloped viruses [1, 8]. In contrast to these studies, our results demonstrated that the sustained release of a significantly lower amount of H_2O_2 (1–5 mM) from DMA-containing microgels was both antimicrobial and antiviral. Most importantly, our microgels reduced the infectivity of the more chemical resistant non-envelope virus by 3 LRV. H_2O_2 solutions have been previously found to be ineffective in inactivating non-enveloped viruses [61] and vaporized H_2O_2 was required to reduce the infectivity of non-enveloped polio virus and norovirus [12, 13]. This is potentially due to the longer half-life of H_2O_2 in vapor than in water. By continuously generating H_2O_2 over time, DMA-containing microgels may have created a similar antipathogenic environment by maintaining an effective H_2O_2 concentration similar to using vaporized H_2O_2 in an enclosed space. Catechol also generates more potent reactive oxygen species such as $O_2^{\bullet -}$, which may have contributed to the enhanced antipathogenic effect [45]. Future studies will be required to determine the ability for DMA-containing microgels to inactivate antibiotic resistant bacterial strains (such as methicillin resistant staphylococcus aureus (MRSA)) and a wider range of viruses. Additionally, the ability to activate the microgels in solutions with complex compositions, such as biological fluid in wounds or solutions with a higher bacterial load like standard drinking water, will be required for applications in the field. Nevertheless, the ability to successfully kill bacteria or inactivate viruses using a very low H_2O_2 concentration is highly attractive as elevated levels of H_2O_2 are cytotoxic and can damage healthy tissue [62, 63].

Recently, H_2O_2–releasing hydrogels have demonstrated antimicrobial property. Lee et. al. [64] utilized H_2O_2 to catalyze tyrosinase-indused crosslinking of tyrosine-conjugated polymer, which released the residual H_2O_2 (0.002–0.5 mM) after the oxidant had catalyzed the crosslinking reaction. Although this hydrogel system exhibited strong antimicrobial property against gram-positive bacteria, H_2O_2 was not generated *in situ*. A carboxymethyl cellulose (CMC)–based hydrogels that contained cellobiose dehydrogenase, an enzyme that catalyze CMC while generating H_2O_2 as a byporduct, demonstrated *in situ* release of 0.03 mM of H_2O_2 for 24 h [65]. This hydrogel inhibited the growth of both *E. coli* and *Staphylococcus aureus*. These hydrogels systems released significantly lower amount of H_2O_2 when compared to DMA-containing microgels, and these previous systems were not designed to repeatedly generate H_2O_2 on command. To our knowledge, our microgel is the first to demonstrate successful inactivation of both non-enveloped and enveloped viruses.

Taken together, we exploited the byproduct generated during a unique redox chemistry found in mussel adhesive proteins for antipathogenic application. The reported microgel generated H_2O_2 on demand when hydrated in an aqueous solution with a neutral to basic pH. The microgels do not contain a reservoir for storing the reactive H_2O_2, which greatly minimizes the potential hazard associated with transporting and storing a highly reactive

oxidation species. These microgels were fabricated using a simple one-step synthetic approach and were easily activated and deactivated in aqueous solutions. The simplicity in fabrication and activation will enable this biomaterial to function as a lightweight and portable source of disinfectant (e.g., instead of large volume of diluted H_2O_2 solution or pressurized gas) for a wide range of applications.

4. Conclusion

In summary, microgels were fabricated with network-bound catechol, which can be activated to generate H_2O_2 on demand. Microgels continuously generated 1–5 mM of H_2O_2 over a period 4 days. The H_2O_2 generation profile can be tuned by the catechol content in the microgel and is dependent on the pH, composition, and temperature of the hydrating fluid. By controlling the oxidation state of the catechol, these microgels can be repeatedly activated and deactivated to generate H_2O_2. Finally, these microgels continuously generated antipathogenic levels of H_2O_2 for killing both gram-positive and gram-negative bacteria and inactivating both enveloped and non-enveloped viruses at H_2O_2 concentrations that were several orders of magnitude lower than previously reported for antipathogenic activity.

Supplementary Material

Refer to Web version on PubMed Central for supplementary material.

Acknowledgements

This work was supported by the National Institutes of Health under award number R15GM104846 (B.P.L.), the Office of Naval Research Young Investigator Award under award number N00014-16-1-2463 (B.P.L.), the Office of the Assistant Secretary of Defense for Health through the Defense Medical Research and Development Program under Award number W81XWH1810610 (B.P.L.), the Portage Health Foundation (B.P.L.), the National Science Foundation under award numbers MDR 1410192 (M.C.F.) and CBET 1451959 (C.L.H.), and the Mack Chair in Bioengineering (C.L.H.). H.M. was supported in part by the Doctoral Finishing Fellowship provided by the Graduate School at Michigan Technological University. The authors acknowledge the Applied Chemical and Morphological Analysis Laboratory at Michigan Tech for use of the instruments and staff assistance.

References

[1]. Abd-Elghaffar AA, Ali AE, Boseila AA, Amin MA, Inactivation of rabies virus by hydrogen peroxide, Vaccine 34(6) (2016) 798–802. [PubMed: 26731189]

[2]. McDonnell G, The Use of Hydrogen Peroxide for Disinfection and Sterilization Applications, PATAI'S Chemistry of Functional Groups, John Wiley & Sons, Ltd 2009.

[3]. Dogan EM, Sudur Zalluhoglu F., Orbey N, Effect of potassium ion on the stability and release rate of hydrogen peroxide encapsulated in silica hydrogels, AIChE Journal 63 (2016) 409–417.

[4]. McDonnell GE, Antisepsis, Disinfection, and Sterilization, American Society of Microbiology 2007.

[5]. Mustafa HSI, <i>Staphylococcus aureus</i> Can Produce Catalase Enzyme When Adding to Human WBCs as a Source of H₂O₂ Productions in Human Plasma or Serum in the Laboratory, Open Journal of Medical Microbiology Vol.04No.04 (2014) 3.

[6]. Presterl E, Suchomel M, Eder M, Reichmann S, Lassnigg A, Graninger W, Rotter M, Effects of alcohols, povidone-iodine and hydrogen peroxide on biofilms of Staphylococcus epidermidis, Journal of Antimicrobial Chemotherapy 60(2) (2007) 417–420. [PubMed: 17586808]

[7]. Thomas EL, Milligan TW, Joyner RE, Jefferson MM, Antibacterial activity of hydrogen peroxide and the lactoperoxidase-hydrogen peroxide-thiocyanate system against oral streptococci, Infection and Immunity 62(2) (1994) 529–535. [PubMed: 8300211]

[8]. Dembinski JL, Hungnes O, Hauge AG, Kristoffersen A-C, Haneberg B, Mjaaland S, Hydrogen peroxide inactivation of influenza virus preserves antigenic structure and immunogenicity, Journal of Virological Methods 207 (2014) 232–237. [PubMed: 25025814]

[9]. McDonnell G, Russell AD, Antiseptics and Disinfectants: Activity, Action, and Resistance, Clinical Microbiology Reviews 12(1) (1999) 147–179. [PubMed: 9880479]

[10]. Tuladhar E, Terpstra P, Koopmans M, Duizer E, Virucidal efficacy of hydrogen peroxide vapour disinfection, Journal of Hospital Infection 80(2) (2012) 110–115. [PubMed: 22153909]

[11]. Heckert RA, Best M, Jordan LT, Dulac GC, Eddington DL, Sterritt WG, Efficacy of vaporized hydrogen peroxide against exotic animal viruses, Applied and Environmental Microbiology 63(10) (1997) 3916–3918. [PubMed: 9327555]

[12]. Montazeri N, Manuel C, Moorman E, Khatiwada JR, Williams LL, Jaykus LA, Virucidal Activity of Fogged Chlorine Dioxide-and Hydrogen Peroxide-Based Disinfectants against Human Norovirus and Its Surrogate, Feline Calicivirus, on Hard-to-Reach Surfaces, Front Microbiol 8 (2017).

[13]. Thevenin T, Lobert P-E, Hober D, Inactivation of an enterovirus by airborne disinfectants, BMC Infectious Diseases 13 (2013) 177–177. [PubMed: 23587047]

[14]. Leigh AG, Stabilization of Hydrogen Peroxide, US, 1981.

[15]. Varma RS, Naicker KP, The Urea–Hydrogen Peroxide Complex: Solid-State Oxidative Protocols for Hydroxylated Aldehydes and Ketones (Dakin Reaction), Nitriles, Sulfides, and Nitrogen Heterocycles, Organic Letters 1(2) (1999) 189–192.

[16]. Li L, Zeng H, Marine mussel adhesion and bio-inspired wet adhesives, Biotribology 5(Supplement C) (2016) 44–51.

[17]. Lee BP, Messersmith PB, Israelachvili JN, Waite JH, Mussel-Inspired Adhesives and Coatings, Annual review of materials research 41 (2011) 99–132.

[18]. Yu M, Hwang J, Deming TJ, Role of L-3,4-dihydroxyphenylanine in mussel adhesive proteins, J. Am. Chem. Soc 121(24) (1999) 5825–5826.

[19]. Rzepecki LM, Waite JH, alpha,beta-Dehydro-3,4-dihydroxyphenylalanine derivatives: rate and mechanism of formation, Arch. Biochem. Biophys 285(1) (1991) 27–36. [PubMed: 1899328]

[20]. Lee BP, Dalsin JL, Messersmith PB, Synthesis and Gelation of DOPA-Modified Poly(ethylene glycol) Hydrogels, Biomacromol 3(5) (2002) 1038–47.

[21]. Forooshani PK, Meng H, Lee BP, Catechol Redox Reaction: Reactive Oxygen Species Generation, Regulation, and Biomedical Applications, Advances in Bioinspired and Biomedical Materials Volume 1, American Chemical Society 2017, pp. 179–196.

[22]. Lee H, Lee BP, Messersmith PB, A reversible wet/dry adhesive inspired by mussels and geckos, Nature 448(7151) (2007) 338–341. [PubMed: 17637666]

[23]. Sambrook J, Molecular cloning : a laboratory manual, Third edition. Cold Spring Harbor, N.Y. : Cold Spring Harbor Laboratory Press, [2001] ©20012001.

[24]. Chapter 4 Reagents, 6th ed., Strasbourg : Council of Europe London, 2008.

[25]. Clement M-V, Long LH, Ramalingam J, Halliwell B, The cytotoxicity of dopamine may be an artefact of cell culture, Journal of Neurochemistry 81(3) (2002) 414–421. [PubMed: 12065650]

[26]. Roy S, Khanna S, Nallu K, Hunt TK, Sen CK, Dermal wound healing is subject to redox control, Molecular therapy : the journal of the American Society of Gene Therapy 13(1) (2006) 211–220. [PubMed: 16126008]

[27]. Häntzschel N, Hund R-D, Hund H, Schrinner M, Lück C, Pich A, Hybrid Microgels with Antibacterial Properties, Macromolecular Bioscience 9(5) (2009) 444–449. [PubMed: 19089873]

[28]. Vilčnik A, Jerman I, Šurca Vuk A, Koželj M, Orel B, Tomšič B, Simončič B, Kovač J, Structural Properties and Antibacterial Effects of Hydrophobic and Oleophobic Sol–Gel Coatings for Cotton Fabrics, Langmuir 25(10) (2009) 5869–5880. [PubMed: 19432495]

[29]. Heldt CL, Hernandez R, Mudiganti U, Gurgel PV, Brown DT, Carbonell RG, A colorimetric assay for viral agents that produce cytopathic effects, J Virol Methods 135(1) (2006) 56–65. [PubMed: 16516983]

[30]. Tafur MF, Vijayaragavan KS, Heldt CL, Reduction of porcine parvovirus infectivity in the presence of protecting osmolytes, Antivir Res 99(1) (2013) 27–33. [PubMed: 23648707]

[31]. Peppas NA, Bures P, Leobandung W, Ichikawa H, Hydrogels in pharmaceutical formulations, Eur. J. Pharm. Biopharm 50(1) (2000) 27–46. [PubMed: 10840191]

[32]. Andreopoulos FM, Beckman EJ, Russell AJ, Light-induced tailoring of PEG-hydrogel properties, Biomaterials 19(15) (1998) 1343–52. [PubMed: 9758034]

[33]. Gudeman LF, Peppas NA, Preparation and Characterization of Ph-Sensitive, Interpenetrating Networks of Poly(Vinyl Alcohol) and Poly(Acrylic Acid), J. App. Polym. Sci 55(6) (1995) 919–928.

[34]. Flory PJ, Rehner J, Statistical mechanics of cross-linked polymer networks. II. Swelling, J. Chemistry Phys 11 (1943) 521–526.

[35]. Pandis C, Spanoudaki A, Kyritsis A, Pissis P, Hernández JCR, Gómez Ribelles JL, Monleón Pradas M, Water sorption characteristics of poly(2-hydroxyethyl acrylate)/silica nanocomposite hydrogels, Journal of Polymer Science Part B: Polymer Physics 49(9) (2011) 657–668.

[36]. Pradas MM, Ribelles JLG, Aroca AS, Ferrer GG, Antón JS, Pissis P, Interaction between water and polymer chains in poly(hydroxyethyl acrylate) hydrogels, Colloid. Polym. Sci 279(4) (2001) 323–330.

[37]. Skelton S, Bostwick M, O'Connor K, Konst S, Casey S, Lee BP, Biomimetic adhesive containing nanocomposite hydrogel with enhanced materials properties, Soft Matter 9(14) (2013) 3825–3833.

[38]. Meng H, Li Y, Faust M, Konst S, Lee BP, Hydrogen peroxide generation and biocompatibility of hydrogel-bound mussel adhesive moiety, Acta Biomaterialia 17 (2015) 160–169. [PubMed: 25676582]

[39]. Halliwell B, Oxidative stress in cell culture: an under-appreciated problem?, FEBS Letters 540(1–3) (2003) 3–6. [PubMed: 12681474]

[40]. Graham DG, Jeffs PW, The role of 2,4,5-trihydroxyphenylalanine in melanin biosynthesis, J. Biol. Chem 252(16) (1977) 5729–34. [PubMed: 195958]

[41]. Rzepecki LM, Waite JH, A Chromogenic Assay for Catecholoxidases Based on the Addition of L-Proline to Quinones, Anal. Biochem 179(2) (1989) 375–381. [PubMed: 2774185]

[42]. Cencer MM, Liu Y, Winter A, Murley M, Meng H, Lee BP, Effect of pH on the rate of curing and bioadhesive properties of dopamine functionalized poly(ethylene glycol) hydrogels, Biomacromol 15(8) (2014) 2861–2869.

[43]. Rzepecki LM, Nagafuchi T, Waite JH, alpha,beta-Dehydro-3,4-dihydroxyphenylalanine derivatives: potential schlerotization intermediates in natural composite materials, Arch. Biochem. Biophys 285(1) (1991) 17–26. [PubMed: 1846730]

[44]. Mochizuki M, Yamazaki S.-i., Kano K, Ikeda T, Kinetic analysis and mechanistic aspects of autoxidation of catechins, Biochimica et Biophysica Acta (BBA) - General Subjects 1569(1–3) (2002) 35–44. [PubMed: 11853955]

[45]. Sawyer DT, Valentine JS, How Super Is Superoxide, Accounts Chem Res 14(12) (1981) 393–400.

[46]. Reznikov K, Kolesnikova L, Pramanik A, Tan-No K, Gileva I, Yakovleva T, Rigler R, Terenius L, Bakalkin G, Clustering of apoptotic cells via bystander killing by peroxides, The FASEB Journal 14(12) (2000) 1754–1764. [PubMed: 10973925]

[47]. Yazici E, Deveci H, Factors Affecting Decomposition of Hydrogen Peroxide, 2010.

[48]. Zhou P, Deng Y, Lyu B, Zhang R, Zhang H, Ma H, Lyu Y, Wei S, Rapidly-Deposited Polydopamine Coating via High Temperature and Vigorous Stirring: Formation, Characterization and Biofunctional Evaluation, PLOS ONE 9(11) (2014) e113087. [PubMed: 25415328]

[49]. Akhtar K, Khalid N, Khan M, Effect of pH and Temperature on the Catalytic Properties of Manganese dioxide, 2012.

[50]. Meng H, Liu Y, Lee BP, Model polymer system for investigating the generation of hydrogen peroxide and its biological responses during the crosslinking of mussel adhesive moiety, Acta Biomater 48 (2017) 144–56. [PubMed: 27744069]

[51]. Jung YS, Lim WT, Park JY, Kim YH, Effect of pH on Fenton and Fenton-like oxidation, Environmental Technology 30(2) (2009) 183–190. [PubMed: 19278159]

[52]. Pizzocaro F, Torreggiani D, Gilardi G, Inhibition of Apple Polyphenoloxidase (Ppo) by Ascorbic-Acid, Citric-Acid and Sodium-Chloride, J Food Process Pres 17(1) (1993) 21–30.

[53]. De Laat J, Le TG, Effects of chloride ions on the iron(III)-catalyzed decomposition of hydrogen peroxide and on the efficiency of the Fenton-like oxidation process, Applied Catalysis B: Environmental 66(1) (2006) 137–146.

[54]. Mirshafian R, Wei W, Israelachvili JN, Waite JH, alpha,beta-Dehydro-Dopa: A Hidden Participant in Mussel Adhesion, Biochem 55(5) (2016) 743–750. [PubMed: 26745013]

[55]. Chelikani P, Fita I, Loewen PC, Diversity of structures and properties among catalases, CMLS, Cell. Mol. Life Sci 61(2) (2004) 192–208. [PubMed: 14745498]

[56]. EPA, Safe Drinking Water Act, 1974.

[57]. FPA, Points to consider in the manufacture and testing of monoclonal antibody products for human use, US Department of Health and Human Services, Rockville, MD, 1997.

[58]. Norkin LC, Virology: Molecular Biology and Pathogenesis, ASM Press 2010.

[59]. Kim I-S, Choi Y-W, Lee S-R, Optimization and Validation of a Virus Filtration Process for Efficient Removal of Viruses from Urokinase Solution Prepared from Human Urine, Journal of Microbiology and Biotechnology 14(1) (2004) 140–147.

[60]. Callens N, Brügger B, Bonnafous P, Drobecq H, Gerl MJ, Krey T, Roman-Sosa G, Rümenapf T, Lambert O, Dubuisson J, Rouillé Y, Morphology and Molecular Composition of Purified Bovine Viral Diarrhea Virus Envelope, PL OS Pathogens 12(3) (2016) e1005476.

[61]. Eterpi M, McDonnell G, Thomas V, Disinfection efficacy against parvoviruses compared with reference viruses, The Journal of hospital infection 73(1) (2009) 64–70. [PubMed: 19646784]

[62]. Brian N, Ahswin H, Smart N, Bayon Y, Wohlert S, Hunt JA, Reactive Oxygen Species (ROS)-A Family of Fate Deciding Molecules Pivotal in Constructive Inflammation and Wound Healing, European Cells and Materials 24 (2012) 249–265. [PubMed: 23007910]

[63]. Loo AEK, Wong YT, Ho R, Wasser M, Du T, Ng WT, Halliwell B, Effects of Hydrogen Peroxide on Wound Healing in Mice in Relation to Oxidative Damage, PLoS ONE 7(11) (2012) e49215. [PubMed: 23152875]

[64]. Lee Y, Choi K-H, Park KM, Lee J-M, Park BJ, Park KD, In Situ Forming and H_2O_2-Releasing Hydrogels for Treatment of Drug-Resistant Bacterial Infections, ACS Applied Materials & Interfaces 9(20) (2017) 16890–16899. [PubMed: 28474514]

[65]. Huber D, Tegl G, Mensah A, Beer B, Baumann M, Borth N, Sygmund C, Ludwig R, Guebitz GM, A Dual-Enzyme Hydrogen Peroxide Generation Machinery in Hydrogels Supports Antimicrobial Wound Treatment, ACS Applied Materials & Interfaces 9(18) (2017) 15307–15316. [PubMed: 28429928]

Statement of Significance

Researchers have designed bioadhesives and coatings using the adhesive moiety catechol to mimic the strong adhesion capability of mussel adhesive proteins. During catechol autoxidation, hydrogen peroxide (H_2O_2) is generated as a byproduct. Here, catechol was incorporated into microgels, which can generate millimolar levels of H_2O_2 by simply hydrating the microgels in a solution with physiological pH. The sustained release of H_2O_2 was both antimicrobial and antiviral, inactivating even the more biocide resistant non-enveloped virus. These microgels can be repeatedly activated and deactivated for H_2O_2 generation by incubating them in solutions with different pH. This simplicity and recyclability will enable this biomaterial to function as a lightweight and portable source for the disinfectant for a wide range of applications.

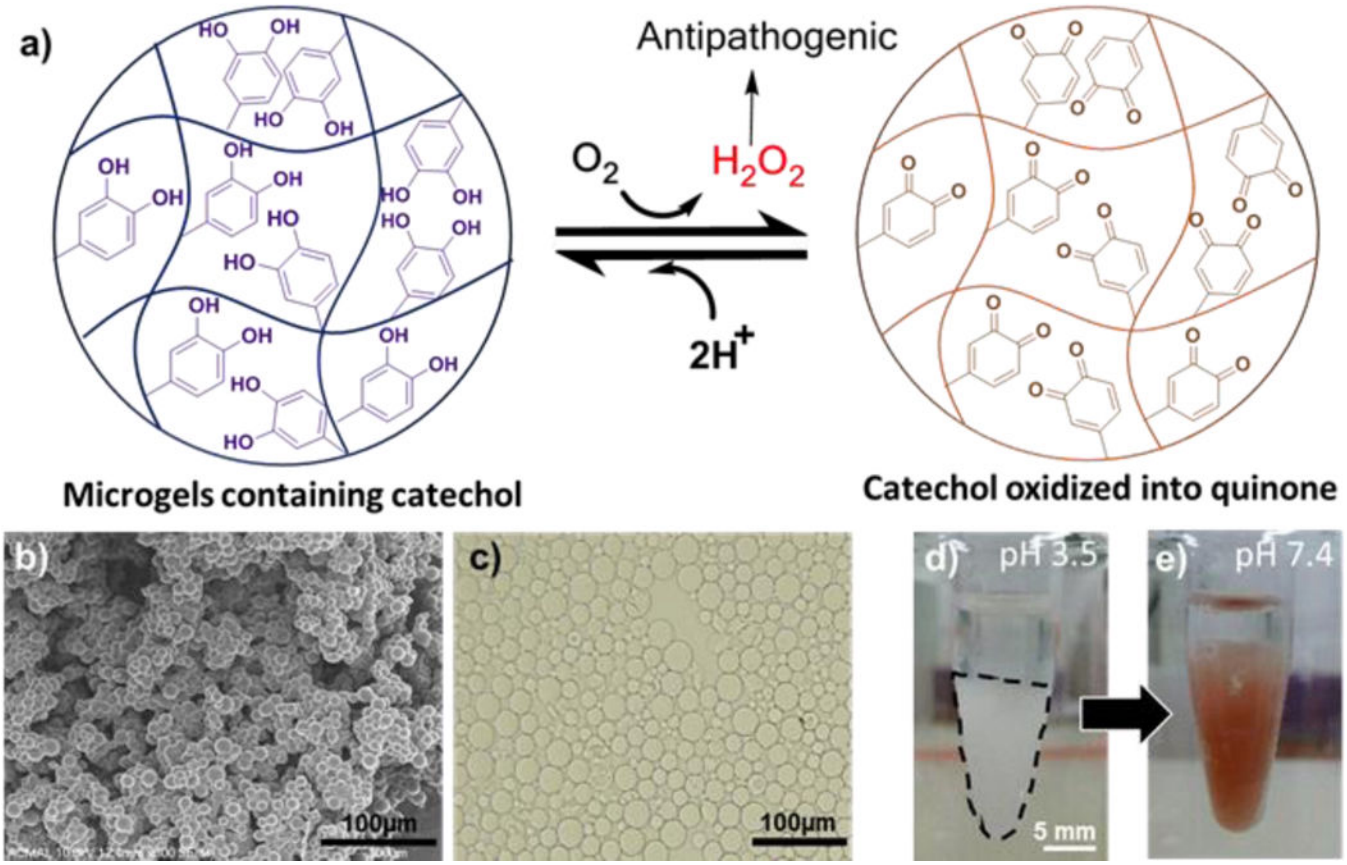

Figure 1.

Catechol-containing microgels generate H_2O_2 during the autoxidation of catechol to form quinone, when the microgel is hydrated in a neutral to basic pH solution (a). SEM (b) and bright-field microscopy (c) images of the dried and hydrated microgels, respectively, confirmed the spherical shape of the microgels. Photographs of the microgels suspended in pH 3.5 DI water (d) and PBS (pH 7.4) (e) indicated that catechol only oxidizes (red color in panel e) in a basic solution. The dashed line in (d) encloses the white, opaque microgels.

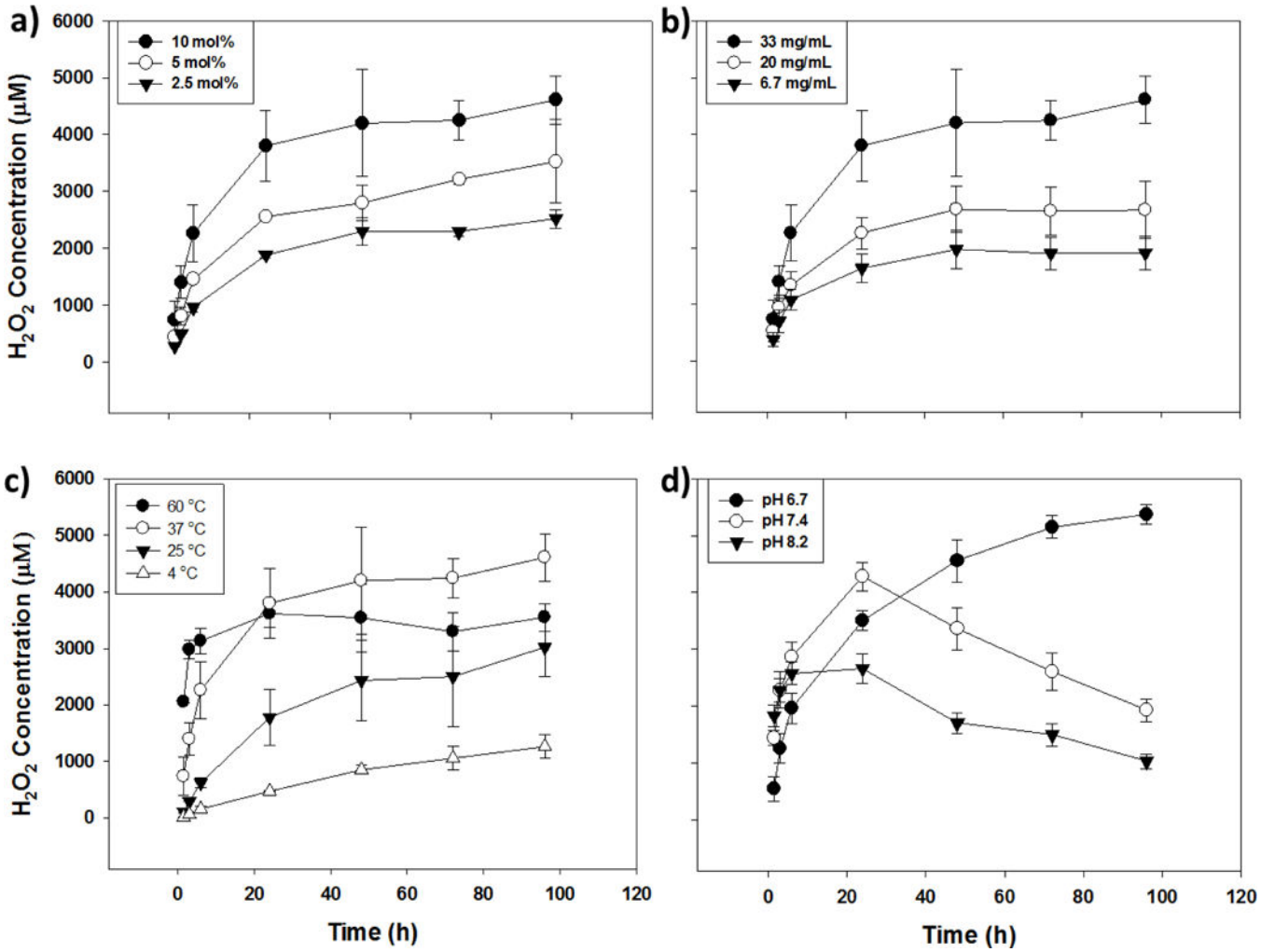

Figure 2.

H_2O_2 generation from 33 mg/mL of microgels with various DMA concentration (0–10 mol %) in PBS (pH = 7.4) at 37°C (a), microgels with 10 mol % DMA at various concentrations (6.733 mg/mL) in PBS (pH = 7.4) at 37°C (b), 33 mg/mL microgels with 10 mol% DMA in PBS (pH = 7.4) at various temperatures (4–60°C) (c), and 33 mg/mL of microgels with 10 mol% DMA in PB with various pH (6.7–8.2) and pH 3.5 DI water at 37°C (d).

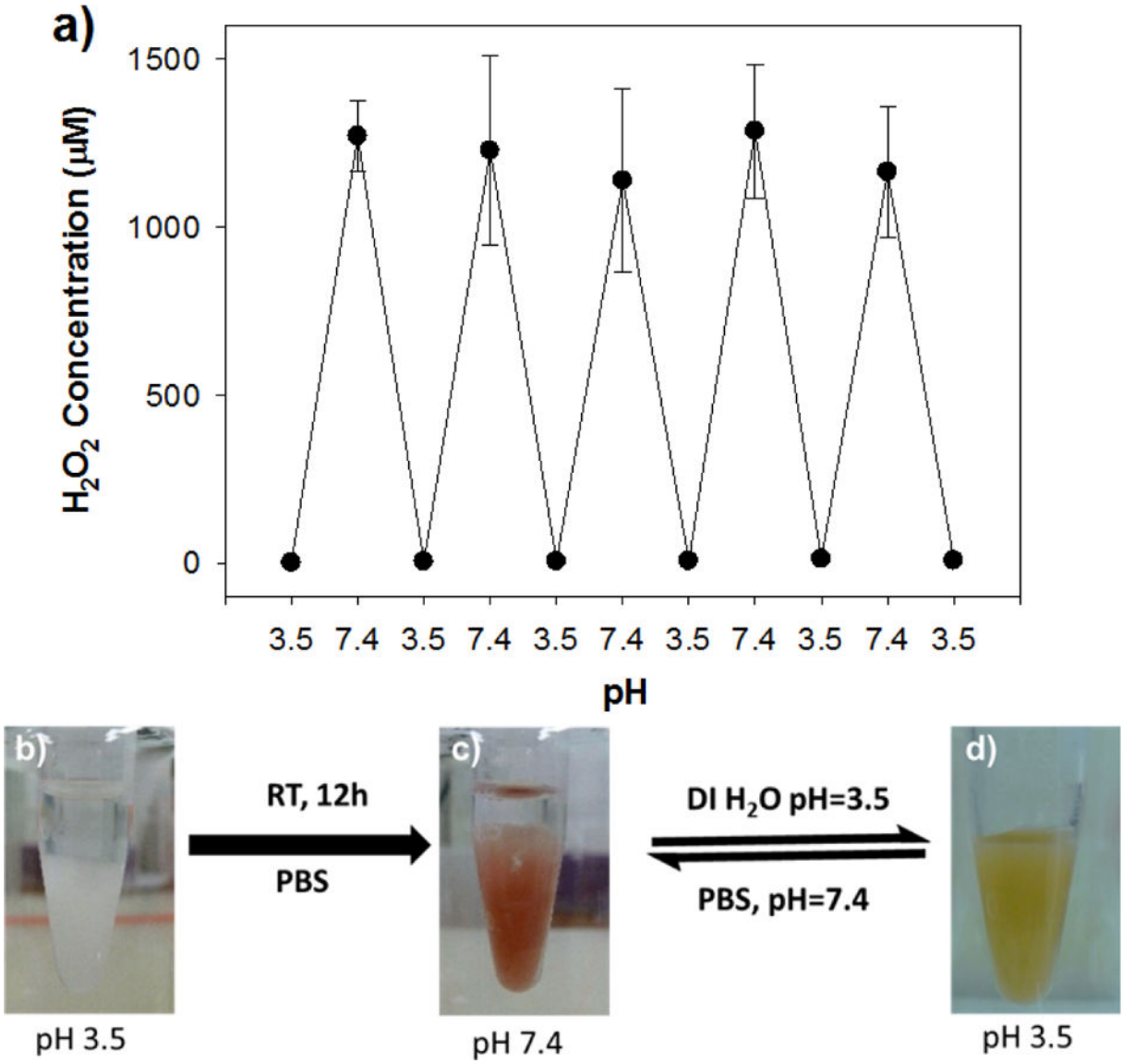

Figure 3.

H_2O_2 generation from 10 mol% DMA-containing microgels when repeatedly incubated at pH 3.5 DI water and pH 7.4 PBS at room temperature (a). H_2O_2 concentration was measured after 12 h of incubation. Photographs of the microgels suspended in pH 3.5 DI water (b) and repeatedly incubated cycled between PBS (pH 7.4) (c) and pH 3.5 DI water (d).

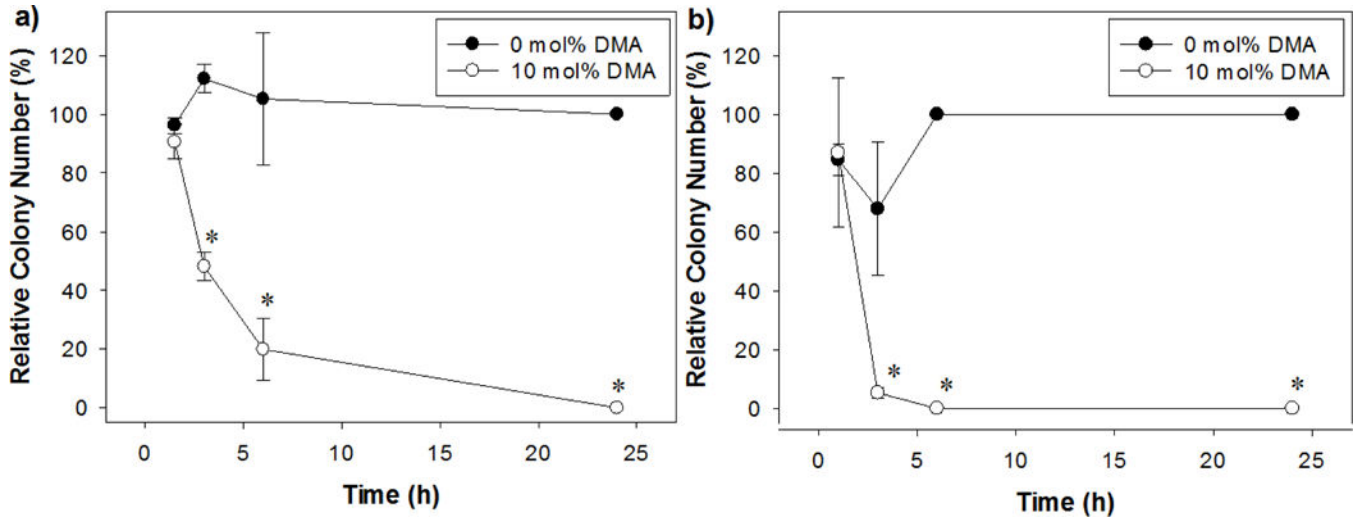

Figure 4.

Relative bacteria colony number for S. epi (a) and E. coli (b) incubated with microgels containing 0 mol% or 10 mol% DMA. The relateive bacteria colony number was normalized by the number of colonies formed by bacteria that were not treated with the microgels. * $p < 0.05$ when compared to microgel containing 0 mol% DMA at a given time point.

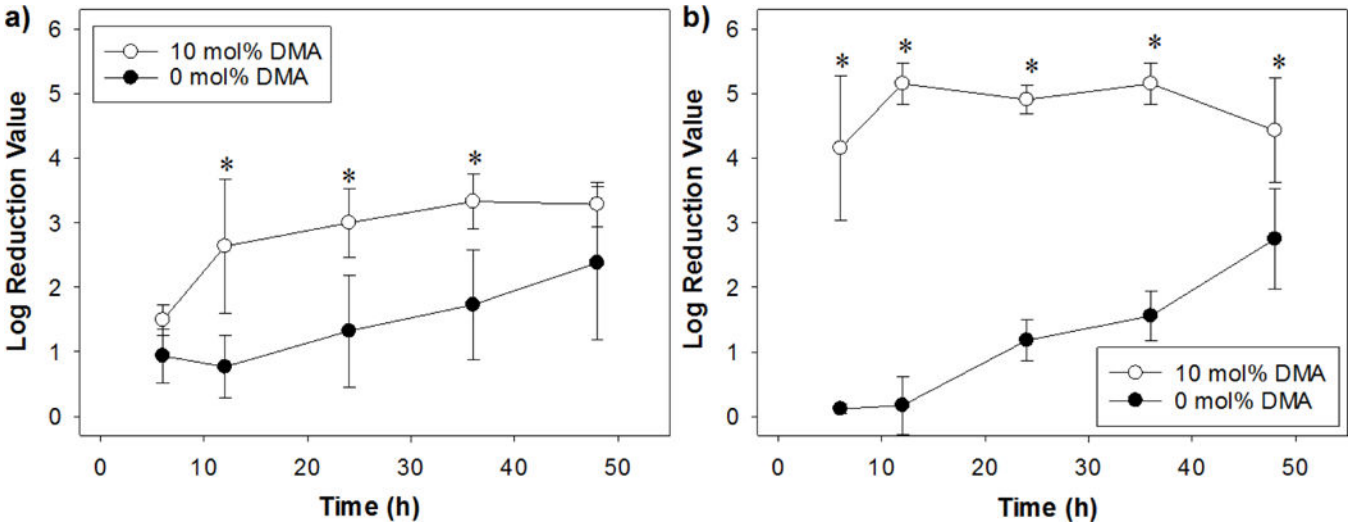

Figure 5.

Log reduction value for PPV (a) and BVDV (b) exposed to microgels containing 0 or 10 mol % DMA with a starting viral titer of 6 log. * $p < 0.05$ when compared to microgel containing 0 mol% DMA at a given time point.

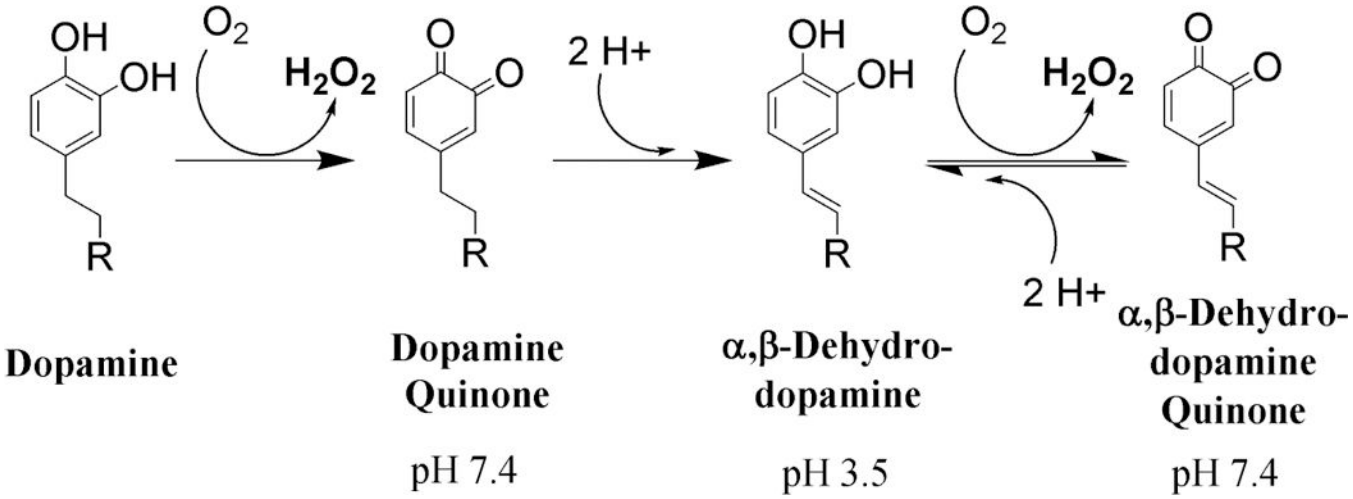

Scheme 1.

Proposed oxidation and reduction of dopamine during repeated cycling of pH. Dopamine is initially transformed into dopamine quinone, which tautomerizes to form α,β-dehydrodopamine. α,βdehydrodopamine regains a catechol moiety that can be further oxidized to α,β-dehydrodopamine quinone, generating H_2O_2 during the process. The subsequent cycling of pH between 3.5 and 7.4 involved the oxidation and reduction of α,β-dehydrodopamine.